COMPARISON OF GROUND MOTION HYBRID SIMULATIONS TO NGA MODIFIED GMPE IN THE MARMARA SEA REGION (TURKEY) IN A DIRECTIVITY RUPTURE CONTEXT

AGU FALL MEETING
San Francisco | 12–16 December 2016
#S31C-2792

M. Pischiutta[1] A. Akinci[1] M. Taroni[1] E. Spagnuolo[1] A. Herrero[1] H. Aochi[2]

1. INGV - Istituto Nazionale di Geofisica e Vulcanologia, Rome (Italy)
2. Risks and Prevention Direction, Bureau de Recherches Géologiques et Minières, Orléans Cedex, France.

We have **simulated strong ground motions** for two Mw>7.0 rupture scenarios on the **North Anatolian Fault,** in the Marmara Sea within 10-20 km of **Istanbul**.This city is characterized by one of the highest levels of seismic risk in Europe and the Mediterranean region. We have considered two right-lateral strike-slip faults oriented N82-90°, dip 90 differing in the position of the enucleation point.
We have implemented an **hybrid approach** merging **low-frequency deterministic modeling** by Aochi & Ulrich (2015) and **high-frequency stochastic simulations** (Akinci et al., 2015).

The **comparison** of intensity measures (PGA, PGV, SA) on our **simulations** with recently proposed regional **ground motion prediction equations** (Boore & Atkinson, 2008), have pointed out the significant role of **rupture directivity and super-shear rupture** effects associated to Mw>7 earthquakes for the Marmara region.

In order **to improve the comparison**, we used the GMPE proposed by Boore & Atkinson (2008) with the **directivity correction proposed by Spudich & Chiou (2008)**. This study highlights the importance of the rupture directivity for the hazard estimation, specifically for the city of Istanbul.

To estimate the ground motion characteristics and its variability in the region we have adopted physics-based rupture scenarios, simulating hybrid broadband time histories. The broadband simulations are implemented as follows:

- Low-frequency seismograms using a full 3D propagation method (Aochi & Ulrich,2015)
- Integrate the dynamically simulated earthquake scenarios adding an additional complexity of k^2 like-slip distribution (Herrero & Bernard 1994)
- High-frequency seismograms using the stochastic finite-fault model (Motazedian & Atkinson,2005)
- More realistic time series by performing a weighted summation at intermediate frequencies to calculate BB signals for 2574 stations every 3 km related to NEHRP A site class

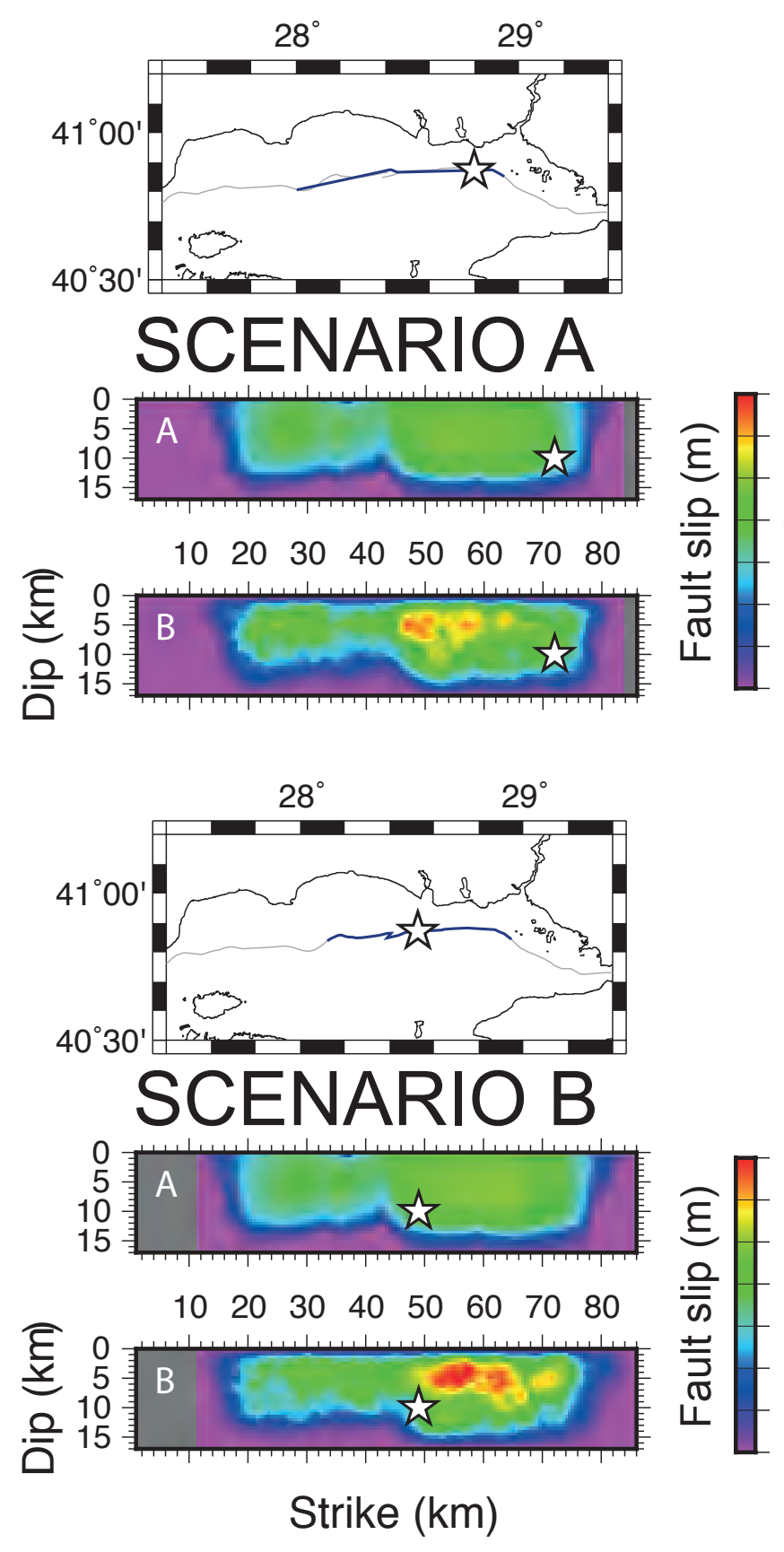

Final slip distributions for the two dynamic rupture models using the k^2slip model along the selected faults. The star depicts the hypocenter location. The Central Marmara Fault CMF and Cinarcik Fault CF segments are given by gray solid line.

Parameter	SCENARIO A	SCENARIO B
Fault orientation (strike & dip)	82°-90°	82°-90°
Fault dimensions	83 x 17 km	74 x 17 km
Moment magnitude	7.26	7.27
Corner of the upper edge (Lat.,Lon.)	40.80 28.00	40.83 28.12
Depth of the top of the fault plane	0 km	0 km
Sub-fault dimensions	1 x 1 km	1 x 1 km
Source spectrum model	Single corner-freq. ω^2	Single corner-freq. ω^2
Stress parameter (bars)	100	100
Shear-wave velocity β (km/s)	3.2	3.2
Density (gm/cc)	2.8	2.8
Rupture propagation speed	0.8β	0.8β
Pulsing area percentage	50%	50%
Geometric spreading, Z(r)	$R^{-1.0}$ for 1<R<40 km $R^{-0.5}$ for R>40 km	$R^{-1.0}$ for 1<R<40 km $R^{-0.5}$ for R>40 km
Attenuation model, Q(f)	$275 f^{-2}$ for f < 0.1 $180 f^{-0.45}$ for f < 0.1	$275 f^{-2}$ for f < 0.1 $180 f^{-0.45}$ for f < 0.1
Source duration	$1/f_a$	$1/f_a$
Distance-dependent duration	0.05R	0.05R
Site amplification	Sarangoni and Hart (1974)	Sarangoni and Hart (1974)
Windowing function	NEHRP A site class (Vs=2950 m/s)	NEHRP A site class (Vs=2950 m/s)
Kappa κ_0 (s)	0.01	0.01

Spectral source parameters used for the High Frequency (HF) Stochastic Ground-Motion Simulations for the two selected earthquakes.

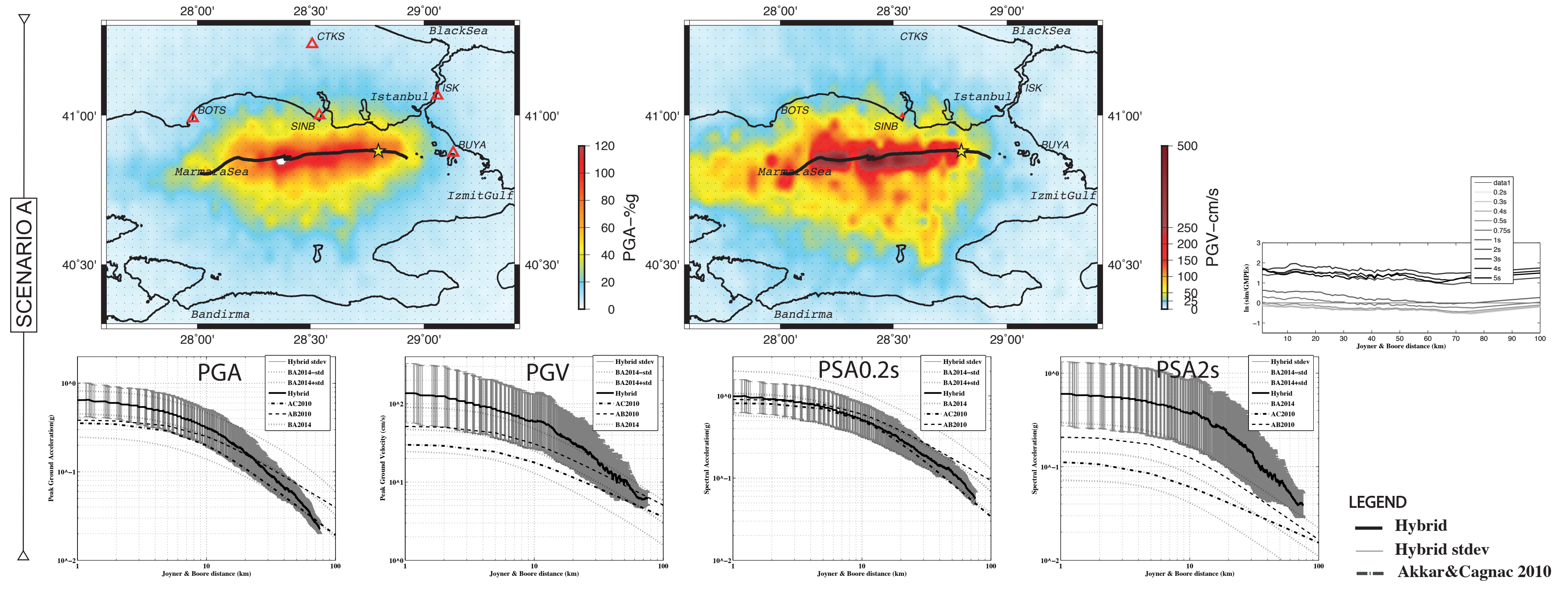

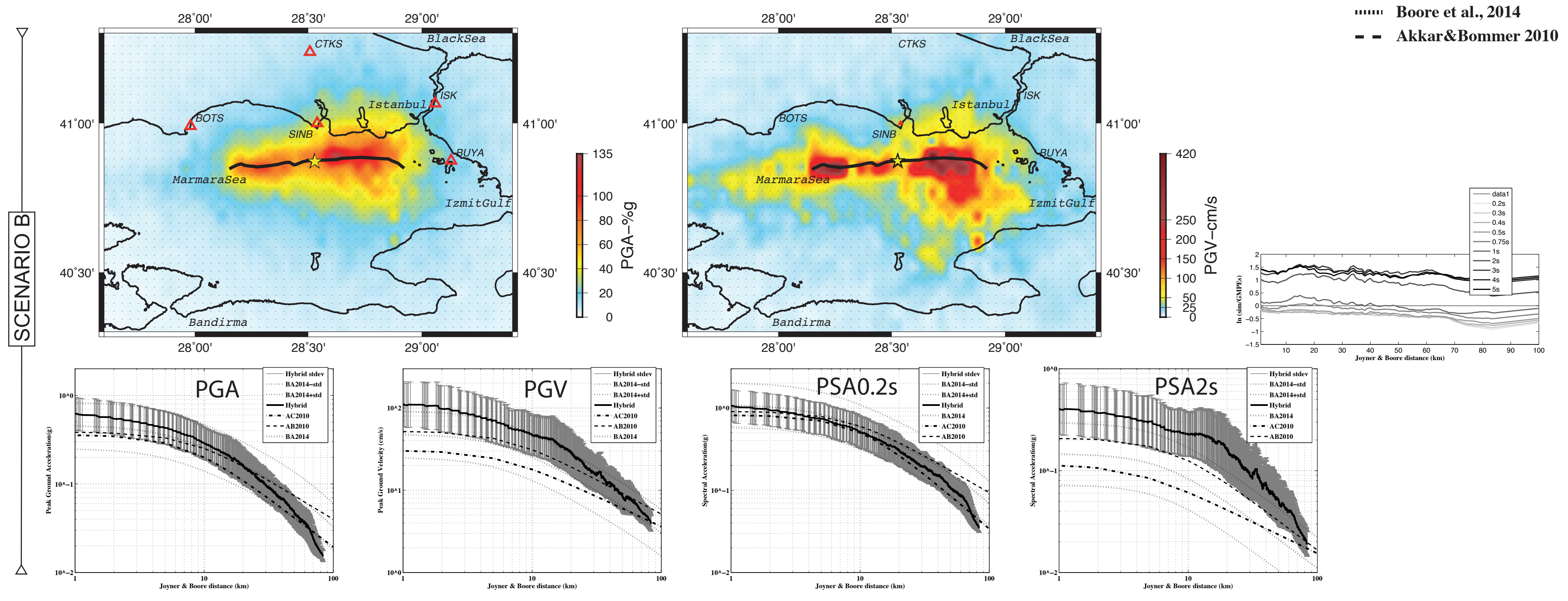

MAIN RESULTS

- High GM parameters are produced in both scenarios due to the higher stress accumulation;
- PGA and PGV distributions are controlled by the slip patches;
- PGV distribution is affected by the rupture directivity;
- High peak velocities far from the fault are caused by super shear rupture;
- GM is consistent with GMPEs for short (PGA) and medium (PGV, PSA 0.2 s) periods. The mean of the simulated PGAs is slightly underestimated at distances larger than 30 km, while they are overestimated at larger (<70 km) distances. At higher periods (PSA 2 s) GM is strongly underestimated by GMPEs.

The **isochrones directivity predictor (IDP)** is calculated considering the source to site geometry, the hypocenter position, a fixed rupture velocity (Vr), rupture direction and focal mechanism.

IDP = S Rri C (Rri - radiation pattern, S - functional form depending on source to site geometry; C - functional form of isochrones velocity C')

c'=[Vs/Vr−(Rhyp−Rrup)/D]^(-1)

(Rhyp - hypocentral distance; Rrup - distance to fault rupture; D - hypocenter and closest point in the source- to-site direction distance)

fD = Tapers(Rrup, M)*(a + b*IDP)

(M - magnitude; a, b empirical constant generally calibrated on specific GMPEs)

In order to improve the comparison between simulated broad band GM levels and GMPE, we apply the correction proposed by Spudich & Chiu (2008) at GMPE by Boore & Atkinson (2008).

For each point of the grid, we compute the probability ratio, i.e. p_corr(Sij) / p(Sij) where Sij is the simulated value at point (i,j) of the spatial grid, p_corr is the gaussian density of the corrected GMPE and p is the gaussian density of GMPE without correction. Values bigger than 1 show that the corrected GMPE works better than the GMPE without correction, while values smaller than 1 show the opposite

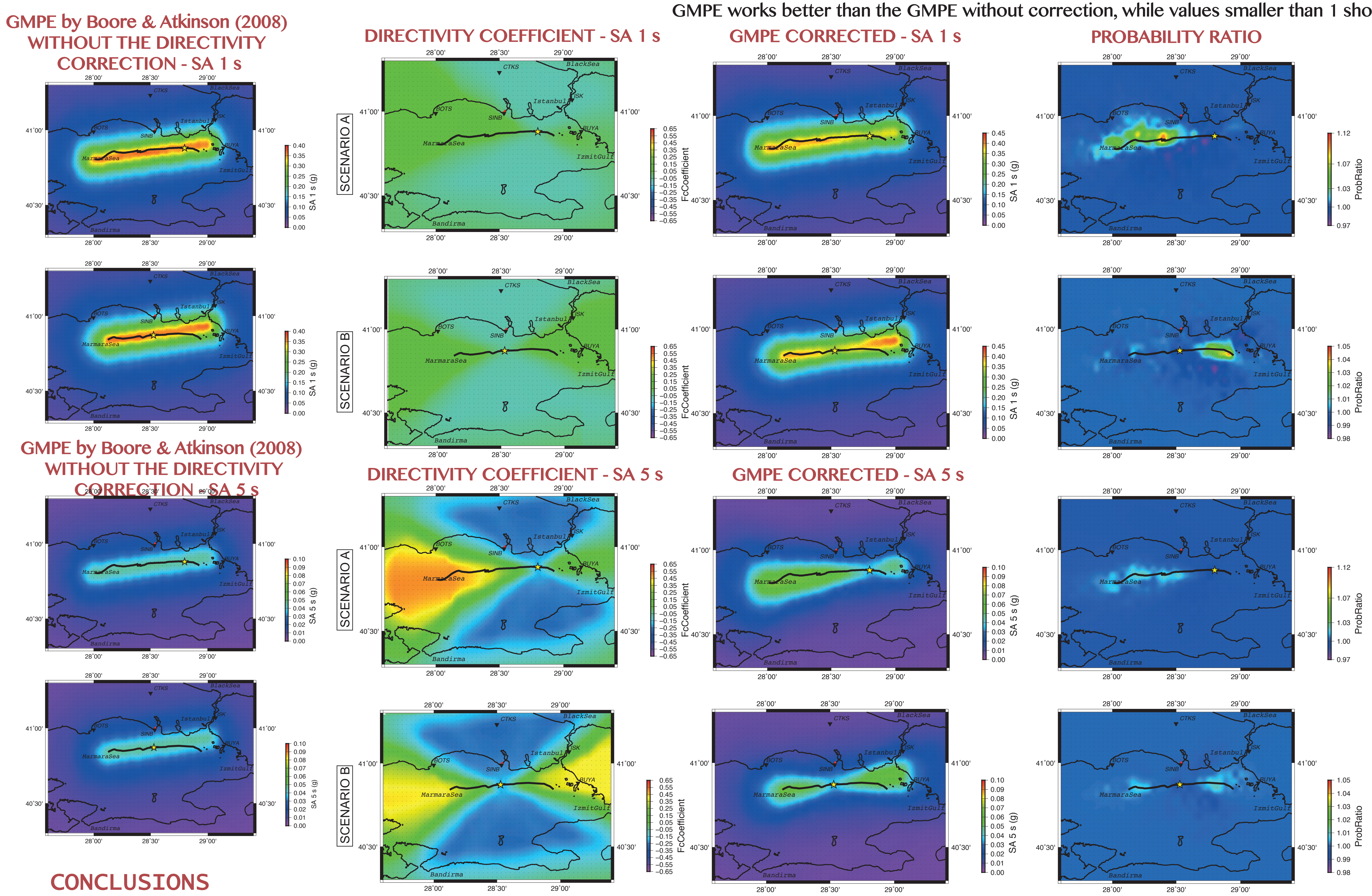

CONCLUSIONS

The directivity effect mostly occurs at high periods, where in our simulation is higher the discrepancy between GMPE and simulated ground motion therefore by applying a directivity correction using the isochrone directivity predictor we did not observe a significant improvement of the discrepancy between GMPE and simulated ground motion. Nevertheless, maps of the probabiity ratio highlight the role of the slip patches, removing the influence of geometrical factors and focal mechanism.